Eur Biophys J (2000) 29: 409–419

ARTICLE

Olivier Thoumine · Jean-Jacques Meister

Dynamics of adhesive rupture between fibroblasts and fibronectin: microplate manipulations and deterministic model

Received: 2 November 1999 / Revised version: 23 March 2000 / Accepted: 19 April 2000

Abstract To characterize the dynamics of cell-substrate adhesive rupture, we used a novel micromanipulation technique, in which individual fibroblasts seized on a rigid microplate were placed into contact with a fibronectin-coated flexible microplate, then pulled away. The fibronectin density (0–3000 molecules/μm^2) and the pulling rate (1–10 μm/s) were controlled. The extent of the contact zone decreased to zero at a time threshold corresponding to adhesive rupture. The uniaxial force at the interface, computed from the deflection of the microplate, increased linearly with time and reached a maximum before dropping to zero. A deterministic model, focusing on the mean number of bonds between fibronectin and its membrane receptor on the cell surface, shows rapid rupture when the force reaches a critical value, in agreement with experimental observations. Increasing the ligand density and the rate of load raises the maximal force (30–200 nN), in reasonably good agreement with the model predictions. Minimization of error between experimental and simulated forces allowed identification of two physicochemical properties of the bond, i.e. its association rate constant ($k_{on}^{2D} = 3 \times 10^{-4}$ μm^2/s) and structural length ($d = 3$ nm). These results may help understand better fibroblast locomotion and interaction with the extracellular matrix.

Key words Micromanipulation · Ligand-receptor interaction

Introduction

Adhesion of cells to the extracellular matrix not only participates in tissue integrity, but also influences cell behavior (e.g. shape, motility, growth, and differentiation) and thus plays a fundamental role in physiology (e.g. neural development and immune responses), repair (e.g. wound healing), and pathology (e.g. metastasis). At the molecular level, cell-matrix adhesion involves specific interactions between extracellular protein ligands, e.g. fibronectin (Mosher 1989) and transmembrane receptors of the integrin family (Hynes 1992). On their cytoplasmic face, integrins bind actin filaments through several proteins, including talin and vinculin (Burridge and Chrzanowska-Wodnicka 1996). Coordinated formation and rupture of adhesive bonds are essential to the control of cell morphology (Davies et al. 1994; Huttenlocher et al. 1995). Such dynamic remodeling of adhesions is regulated by chemical events (e.g. phosphorylation) and by mechanical factors, in particular cytoskeletal tension (Crowley and Horwitz 1995). Tension is generated through contractile actin-myosin stress fibers (Kreis and Birchmeier 1980), and transmitted to the extracellular matrix through integrins (Ingber 1991). Rupture of adhesive sites at the rear upon cytoskeletal contraction is essential for fibroblasts to move forward (Regen and Horwitz 1992; Lauffenburger and Horwitz 1996). Thus, it is important to understand on a physical basis how cell-matrix contacts rupture under stress.

One way to address this issue in vitro is to impose external forces to adherent cells until they separate from a ligand-coated substrate (Hubbe 1981; Bongrand et al. 1994). Several experiments of this type, using techniques of centrifugation (McClay et al. 1981; Hertl et al. 1984; Lotz et al. 1989; Thoumine et al. 1996), hydrodynamic flow (Mohandas et al. 1974; Mège et al. 1986; Truskey and Pirone 1990; Palecek et al. 1997), and micropipet manipulation (Evans et al. 1991; Tözeren et al. 1992; Sung et al. 1994), have led to estimation of kinetics of detachment and rupture forces. The latter range from 10^{-10} N to 10^{-7} N, scatter being due to differences at several levels: (1) type of cell, each possessing specific structural and mechanical properties; (2) type, number, and mobility of receptor and ligand molecules involved in adhesion; (3) cell deformation and active force

O. Thoumine · J.-J. Meister (✉)
Biomedical Engineering Laboratory,
Swiss Federal Institute of Technology,
1015 Lausanne, Switzerland
e-mail: Jean-Jacques.Meister@epfl.ch

generation (e.g. traction); (4) temperature, likely to affect many processes (cytoplasm viscosity, kinetic rates of molecular reactions); (5) type, direction, rate and duration of force applied. One way to better interpret such experiments and allow identification of important molecular parameters in adhesion is to use mathematical modeling.

Several models of cell adhesion have been formulated, which fall into three main categories (Lauffenburger and Linderman 1993): thermodynamic (Bell et al. 1984), mechanical (Evans 1985; Dembo et al. 1988; Tözeren 1990; Ward et al. 1995), and statistical (Cozens-Roberts et al. 1990; Truskey and Pirone 1990). Typically, these models predict how some measurable quantity characterizing adhesion (area and profile of cell-substrate contact zone, peeling velocity, fraction of adherent cells) depends on the imposed experimental conditions, e.g. ligand density, temperature, time, and force, through parameters related to the molecular interaction, e.g. chemical affinity between receptor and ligand, range of the bond, and adhesion energy. One important issue in these approaches is the link between the mechanics and chemistry of the molecular complex. In particular, if one considers the receptor-ligand interaction as a chemical reaction with characteristic association and dissociation rates, how are these parameters affected by a force placed on the bond? Several expressions have been proposed to describe the influence of force on these kinetic rate constants (Bell 1978; Dembo et al. 1988; Evans et al. 1991; Evans and Ritchie 1997), some of which have been verified experimentally (Alon et al. 1995; Piper et al. 1998).

A lot of recent work has focused on the physical properties of selectin-based interactions, particularly in the context of leucocyte rolling on the endothelium (Kaplanski et al. 1993; Alon et al. 1995). However, little is known on the mechanics of molecular interactions with the extracellular matrix. In this context, the objective of our study was to measure some physicochemical characteristics of the fibronectin-integrin bond. On the experimental side, we used microplate manipulation to separate individual fibroblasts from fibronectin-coated glass, allowing precise quantification of the force and contact area during adhesion rupture. On the theoretical side, we used a deterministic model which predicts the average number of receptor-ligand bonds over time. By fitting the data, we obtained the association rate constant and the structural length of the bond.

Materials and methods

Cell culture

NIH mouse 3T3 fibroblasts were generously provided by C. Ruegg (ISREC, Epalinges, Switzerland). Cells were fed with Dulbecco's modified Eagle's medium supplemented with 10% fetal bovine serum and 0.05% gentamycin. Cell culture reagents were purchased from Seromed (Germany).

Microinstrument preparation

Microplates were fabricated from $0.1 \times 1 \times 100$ mm borosilicate bars (VitroCom, Mountain Lakes, NJ, USA) using a micropipet puller (Sutter Instruments, Novato, Calif., USA). By adjusting the parameters of the puller, two types of microplates were made (Fig. 1): (1) rigid ones, with stiffness (taken as the force divided by the deflection of the tip) of about 10^{-6} N/μm, and (2) more flexible ones (stiffness between 10^{-9} and 10^{-8} N/μm). Before manipulation, rigid microplates were cleaned with sulfochromic acid (Merck), silanated, and treated with glutaraldehyde as described (Thoumine and Ott 1997a), to produce a strongly adhesive surface necessary to hold cells (covalent bonds are formed between membrane proteins and the glass surface). Flexible microplates were coated with bovine fibronectin by incubation for 1 h at room temperature in solutions of 0, 0.3, 1, 3, or 10 μg/ml in PBS, and rinsed in PBS right before use. Unless otherwise indicated, chemicals were purchased from Sigma (St. Louis, Mo., USA).

Quantification of fibronectin density

The surface density of fibronectin adsorbed on microplates was assumed to be equal to that on glass coverslips. The latter was determined as described (Thoumine et al. 2000) and found to be proportional to the fibronectin concentration used for incubation, 10 μg/ml corresponding to approximately 3000 molecules/μm^2.

Instrumentation

Microplates were fixed to steel arms and maneuvered using two 30-mm mechanical micromanipulators (Physik Instrumente, Waldbronn, Germany), mounted on each side of the stage of an inverted microscope (Zeiss, Germany) placed on an anti-vibration table (TMC, Peabody, Mass., USA). Fine displacement of the rigid microplate (Fig. 1) was achieved using a 25-μm range piezoelectric translator (Piezomike, Physik Instrumente) controlled by a computer (Power Macintosh, Apple) through a digital-analog interface (LabView software, National Instruments, Austin, Tx., USA).

Cell manipulation

Cells from a 1 cm^2 culture well were detached using 0.005% trypsin-20 mM EGTA in McCoy's 5A medium lacking Ca^{2+}, resuspended in MEM-Hepes, and added to the manipulation chamber. One fibroblast was captured on a rigid microplate, as described (Thoumine and Ott 1997a). After 5 min, the medium was replaced by MEM-Hepes containing 10% FBS, and the cell was transferred in a CO_2 incubator at 37 °C and allowed to spread for 1 h (Thoumine et al. 1999a, b). The cell was then brought back to the microscope. The microplate was turned by a 90° angle (Fig. 2A), and the cell was pushed by about 2 μm against a fibronectin-coated flexible microplate (Fig. 2B), so as to force adhesion. After a 5 min incubation, the rigid microplate was displaced by 25 μm linearly

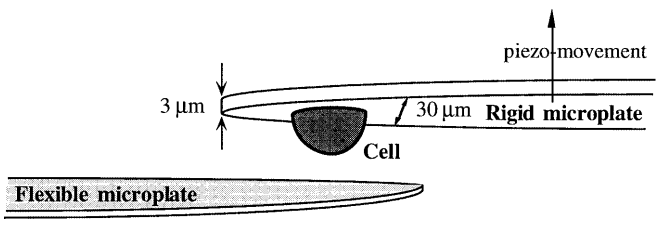

Fig. 1 Perspective drawing of the experiment. The rigid microplate is coated with glutaraldehyde and the flexible one with fibronectin

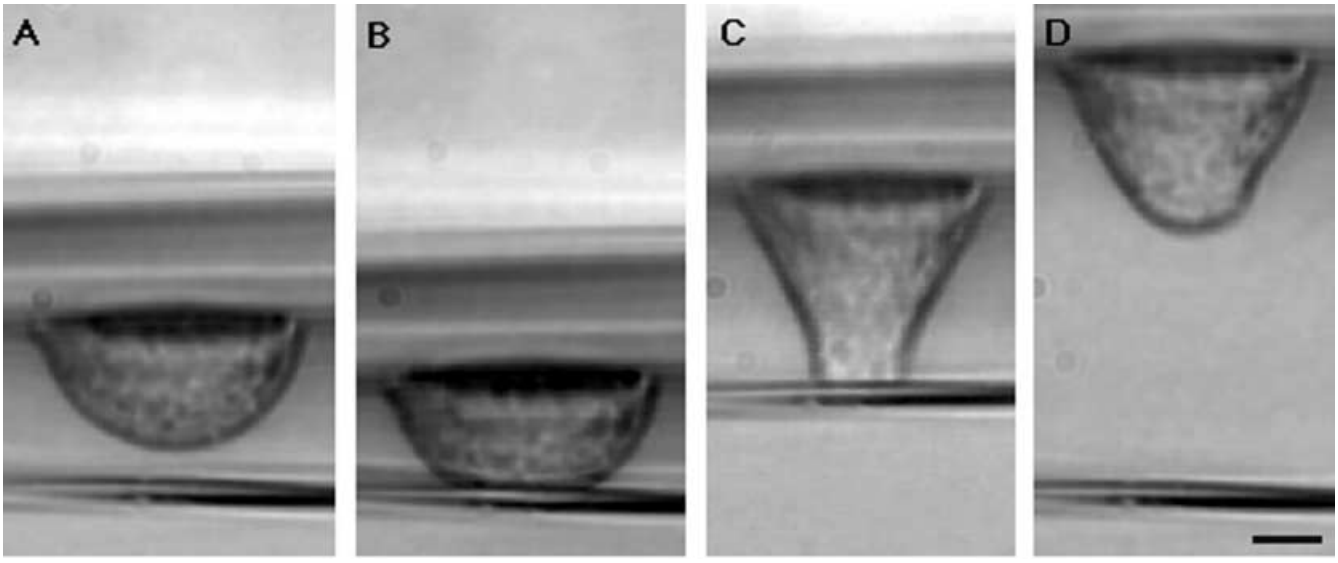

Fig. 2A–D Detachment test. **A** A fibroblast (center) captured and slightly spread on a rigid microplate (top contour) was placed into contact with a fibronectin-coated (1000 molecules/μm^2), flexible microplate (bottom contour), and incubated for 5 min. A slight compression was imposed. The cell in **B** is shown at the end of the adhesion period. The rigid microplate was then displaced upward by 25 μm in 10 s. The cell is shown right before (**C**) and after (**D**) adhesion rupture, which occurred in this case at $t_c = 6$ s. Note the deflection of the flexible microplate. Cells are viewed from the side. *Bar*, 5 μm

with time, using the piezoelectric translator (Fig. 2C). The duration of the displacement was either 3, 10, or 30 s. The stiffness of the flexible microplate was adjusted with respect to the fibronectin concentration so that adhesive rupture occurred within the given time period (Fig. 2D). In some cases, 400 μg/ml Gly-Arg-Gly-Asp-Thr-Pro (RGD) peptides were added to the suspension. All experiments were performed at room temperature (23 °C).

Force calibration

At the end of each experiment, a reference microplate was placed onto the tip of the flexible microplate and moved linearly by 25 μm in 20 s. The relationship between the deflections of the two instruments was linear, allowing determination of the flexible microplate rigidity. To estimate its stiffness, the reference microplate was previously coated with 10 μg/ml fibronectin and used to capture a cell. It was turned by 90°, giving a side view of the cell, and a micropipet (internal diameter on the order of 6 μm) was approached from the free extremity of the cell. Micropipets were pulled and bent to 90° as described (Thoumine et al. 1999a). Negative pressure in the pipet was increased by 10 mm H_2O increments (up to 100 mm H_2O), and the pipet was displaced at a speed of 2 μm/s. At a certain point during pulling, cells slipped out of the pipet: the force at the basal surface (microplate stiffness times deflection) was then equal to the force at the apical side (pressure times pipet cross section). The relationship between the measured deflection and the apical force was linear (Thoumine et al. 1999b), the slope of which being taken as the microplate stiffness, k (between 10^{-9} and 10^{-8} N/μm).

Image acquisition and analysis

Cell-substrate separation was filmed under bright-field illumination using a 40 × /0.75 objective, a 1.6× Optovar lens, and a CCD camera (Cohu, San Diego, Calif., USA) connected to an sVHS video cassette recorder (Sanyo, Japan). Videotapes were played back and images were digitized with a personal computer (Power MacIntosh, Apple) equipped with a frame grabber card (Scion, Frederick, Md., USA). Using image processing software (NIH Image 1.60), the following parameters were measured over time (t): (1) the diameter of conjugation between the cell and the flexible microplate (D); and (2) the deflection of the flexible microplate (δ). Errors, taking into account optical resolution and low frequency vibrations, were on the order of 0.4 μm. The apparent contact area was computed as $A_c = \pi D^2/4$. The instantaneous peeling velocity was taken as the difference in contact diameter between two subsequent time points, divided by the time interval. The force applied on the cell was calculated by multiplying the microplate deflection by its stiffness obtained from the calibration procedure ($F = k\delta$). Deflection of the rigid microplate, around 100 times stiffer than the flexible instrument, was neglected. The error on force measurements, including detection of the microplate position, thermal drift of the instruments, and calibration procedure, was about 15%. We also measured the total apparent cell area (A_T) at the end of the adhesion phase, using a program added to NIH Image, described elsewhere (Thoumine et al. 1999a, b). Apparent areas (A_c and A_T) in moderately spread fibroblasts are slightly lower than actual surface areas (30% at the most), because of membrane wrinkles (Thoumine et al. 1999a).

Characterization of the proteins present in the contact zone

To analyze the material left behind on the flexible microplate after cell separation, immunofluorescent staining was carried out directly in the chamber, essentially as described (Thoumine and Ott 1996), using the following primary antibodies (20 μg/ml): rabbit anti-human fibronectin, mouse anti-chick β_1 integrin, rabbit anti-mouse α_5 integrin, or rabbit anti-human β_1 integrin (Chemicon, Harrow, UK). These antibodies were species cross-reactive. Secondary antibodies were TRITC-labeled goat anti-rabbit or anti-mouse IgG. Observation was made under epifluorescence illumination with a 63×/1.25 oil objective.

Theoretical analysis

Model hypotheses

Cell-substrate adhesion was considered to rely on the specific interaction between a ligand (fibronectin) and its receptor, e.g. the

$\alpha_5\beta_1$ integrin (Hynes 1992), taken as a first-order reversible chemical reaction:

$$R + L \underset{k_{off}}{\overset{k_{on}}{\rightleftharpoons}} R \cdot L$$

where R is the free receptor, L the free ligand, and $R \cdot L$ the complex (noted C). The reaction is driven by two kinetic parameters, the 2D rate of association k_{on}^{2D} ($\mu m^2/s$) and the rate of dissociation k_{off} (s^{-1}). The number of specific bonds was relatively high in our experimental conditions since the forces to separate cells from the microplates were 3–4 orders of magnitude larger than the strength of a single fibronectin-integrin bond (Thoumine et al. 2000). Thus, we adopted a deterministic framework, reasoning on the mean number of bonds.

Attachment phase

For the attachment period, the area of the contact zone (A_c) and the parameters k_{on}^{2D} and k_{off} were taken as constants, i.e. $k_{on}^{2D} = k_{on}^{2D\,0}$ and $k_{off} = k_{off}^0$, respectively, where the superscript means that the tensile force on the bonds is zero. The time rate of change of the bond number (C) is given by:

$$dC/dt = k_{on}^{2D} LR - k_{off} C \quad (1)$$

The free ligand density (molecules/μm^2) is:

$$L = N_L - C/A_c \quad (2)$$

where N_L is the total density of ligand immobilized on the substrate. Neglecting protein diffusion into the contact zone, the conservation of receptors reads:

$$R + C = R_T(A_c/A_T) \quad (3)$$

with R_T the total number of receptors on the cell surface and A_T the total cell area. This approximation is based on the fact that fibronectin receptors move quite slowly in the membrane, i.e. with diffusion coefficient D around 0.03 $\mu m^2/s$ (Duband et al. 1988; Choquet et al. 1997). Thus, during the incubation period $t_a = 5$ min, only receptors situated at a distance lower than $(2Dt_a)^{1/2} = 4$ μm from the contact zone will move into it by diffusion, corresponding to a surface area around 180 μm^2, i.e. about $A_T/6$. This is an upper estimate since short-term motion of membrane proteins is generally restricted to domains of about 1 μm in size, because of so-called barriers to diffusion, e.g. owing to cytoskeletal constraints (Sheetz 1993). It is also probable that receptors move in and out of the contact area in an equilibrium fashion, thus reducing selective trapping of receptors there. Adhesion receptors have indeed been shown to accumulate into contact zones only at longer time scales (Dustin et al. 1996) and in biological systems where diffusion (i.e. that of Fc receptors) is 10-fold faster (Michl et al. 1983; McCloskey and Poo 1986).

We now introduce five dimensionless variables and parameters (Cozens-Roberts et al. 1990):

(1) Fraction of occupied receptors: $\theta = C/R_T$
(2) Dimensionless time: $\tau = k_{on}^{2D} N_L t$
(3) Bond affinity: $\kappa = k_{off}^0/k_{on}^{2D} N_L$
(4) Relative contact area: $\sigma = A_c/A_T$
(5) Ratio of receptor to ligand: $v = R_T/N_L A_c$

By introducing expressions (2) and (3) into Eq. (1), we obtain in dimensionless form:

$$d\theta/d\tau = (1 - v\theta)(\sigma - \theta) - \kappa\theta \quad (4)$$

With the initial condition of no bond, $\theta(0) = 0$, the solution of Eq. (4) is:

$$\theta(\tau) = \frac{\theta_1\left(1 - e^{v(\theta_1-\theta_2)\tau}\right)}{(1 - (\theta_1/\theta_2)e^{v(\theta_1-\theta_2)\tau})} \quad (5)$$

θ_1 and θ_2 being the two roots of the second-degree equation: $\theta^2 - (1 + \kappa + \sigma v)\theta + \sigma = 0$, with $\theta_1 > \theta_2$. The non-dimensional bond number θ increases with time, reaching a plateau value θ_{eq} at $\tau \to \infty$. As an example, increasing the bond affinity (i.e. decreasing κ) accelerates the dynamics and raises the plateau value (Fig. 3A). At low ligand density, θ_{eq} is between zero and $1/v = N_L A_c/R_T$, i.e. the dimensionless number of ligands in the contact zone (ligand-limited regime). At high ligand density, θ_{eq} approaches $\sigma = A_c/A_T$, i.e. the relative number of receptors in the contact zone (receptor-limited regime).

Detachment phase

At the end of the attachment period [$t_a = 5$ min, $\theta(t_a) = \theta_a$], a tensile force varying linearly with time ($F = F't$) was imposed on the adhesive zone. We suppose that bonds are uniformly distributed in the contact area, which is realistic since ligand molecules stick randomly on the substrate. We further assume that the overall force, F, acting on the cell is equally shared by all bonds (Hammer and Lauffenburger 1987). An alternative view would be that the stress is concentrated at the periphery of the contact zone. The choice between those two possibilities essentially depends on the type of mechanical model used to describe the fibroblast structure: either a homogeneous viscoelastic material (Thoumine and Ott 1997a) or a viscous core bounded by an elastic cortex with a rest tension (Thoumine et al. 1999a), respectively. Since it is difficult at the present time to discriminate beween these two

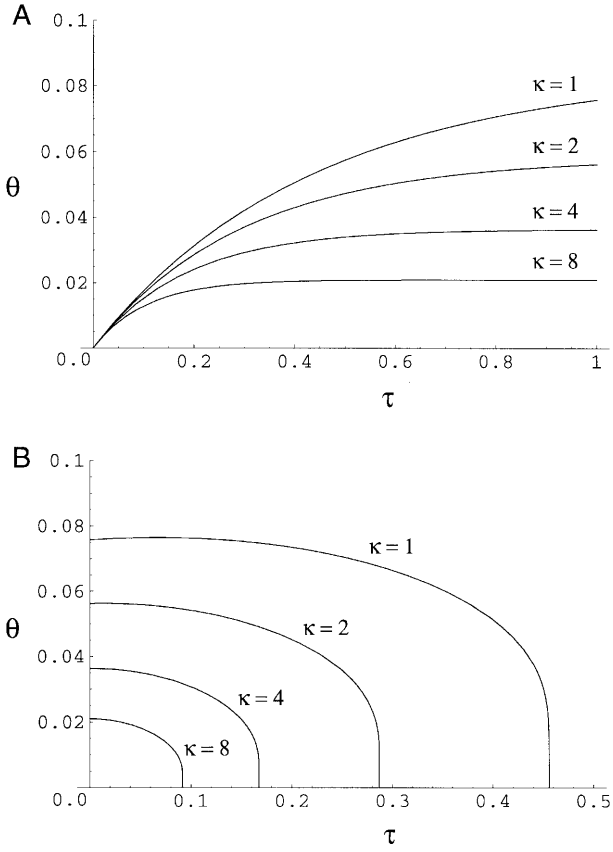

Fig. 3A, B Simulation of adhesive behavior. The fraction of occupied receptors (θ) versus dimensionless time (τ), for various values of the parameter κ (the inverse of bond affinity). **A** Attachment phase, **B** detachment phase. Parameters were chosen as in Table 1, giving the following groups: $\alpha = 0.25$, $\sigma = 0.2$, and $v = 3$. Note that θ drops to zero at a critical time

models, we pick here the simplest case, i.e. that of uniform stress. In addition, the association rate (k_{on}^{2D}) and the contact area (A_c) were again considered as constant. The latter assumption is actually in conflict with experiments, which show a dramatic decrease in contact diameter during cell detachment (actually characterizing adhesive rupture). However, allowing A_c to decrease would probably not affect much the rapid divergence of Eq. (7) (see below), which is dominated by the exponential term (A_c only alters parameters σ and v, and in opposite ways, so the polynomial term stays roughly constant).

Following Bell (1978), the dissociation rate was hypothesized to depend on force through the following relationship:

$$k_{off} = k_{off}^{0} \exp(fd/k_B T) \quad (6)$$

where f is the tensile force acting on one bond ($f = F/C$), d is a characteristic structural length of the receptor-ligand bond, k_B is Boltzmann's constant, and T the absolute temperature. The term in the exponential may be viewed as the ratio between the elastic energy stored by the bond (fd), and the thermal energy. Measurements of the dissociation rate of single bonds between selectins and their carbohydrate ligands (Alon et al. 1995; Piper et al. 1998) recently gave some credit to this formulation. Introducing a dimensionless parameter for the rate of force:

$$\alpha = F' d/(k_B T k_{on}^{2D} N_L R_T)$$

the evolution of the relative number of bonds is given by:

$$d\theta/d\tau = (1 - \nu\theta)(\sigma - \theta) - \kappa\theta e^{\alpha t/\theta} \quad (7)$$

Equation (7) was integrated numerically using commercially available software (Mathematica 3.0, Wolfram Research) run on a personal computer (Power MacIntosh, Apple), with the initial condition $\theta(0) = \theta_a$. Results from the simulations are shown in Fig. 3B, with parameters given in Table 1. For all sets of parameters tested, θ remains fairly constant before a time threshold, t_c, is reached, at which the fraction of bonds decreases catastrophically to zero. This event is interpreted as adhesive rupture. For a constant force and neglecting ligand depletion, the search for a steady state ($d\theta/d\tau = 0$) shows the existence of a critical force above which bond rupture occurs systematically (Bell 1978; Cozens-Roberts et al. 1990). Here, since the force increases linearly with time, it always ends up reaching this threshold for detachment. By multiplying the loading rate by the critical time, one obtains a maximal force $F_{max}^{sim} = F' t_c$, taken as the adhesive strength of the cell. In practice, F_{max}^{sim} is computed for different sets of parameters and expressed versus the ligand density or the loading rate, the main control variables in our experiments. For example, increasing α (e.g. by raising the loading rate F' or the bond interaction distance d) or v (e.g. by compressing the cell to raise the contact area A_c, or by decreasing the ligand density N_L) both reduce θ_a and t_c (not shown). In contrast, θ_a and t_c increase with bond affinity, i.e. decreasing κ.

Table 1 Estimated parameter values and measured variables

Parameter	Notation	Value range
Association rate[a]	k_{on}^{2D}	10^{-9}–10^{-4} μm²/s
Dissociation rate[a]	k_{off}^{0}	0.15 s^{-1}
Bond structural length[b]	d	0.1–10 nm
Receptor number[c]	R_T	500,000
Ligand density[d]	N_L	0–3000 molecules/μm²
Contact area[d]	A_c	181 ± 85 μm²
Total area[d]	A_T	1081 ± 298 μm²
Temperature[d]	T	298 ± 2 K
Rate of force[d]	F'	10^{-9}–10^{-7} N/s
Detachment time[d]	t	3–30 s

[a] The whole-cell association rate of fibroblasts to fibronectin is a lumped parameter $k_+ = k_{on}^{2D} R N_L$, where R is the number of receptors capable of binding. k_+ is in the range of 0.3–1.5 s^{-1} for N_L = 100–3000 molecules/μm² (Thoumine et al. 2000). Boundary values for k_{on}^{2D} are computed for $R = R_T$ (all receptors on the cell surface can interact), and $R = R_T A_c/A_T$ (only the receptors in the contact area can bind), with A_c = 0.2 μm² (value at low compressive force). The dissociation rate k_{off}^{0} was found relatively independent of ligand density and compression

[b] Bell (1978); Erickson (1994); Alon et al. (1995); Piper et al. (1998)

[c] Akiyama and Yamada (1985); Codogno et al. (1987)

[d] This study

Results

Qualitative assessment of adhesive rupture

Individual fibroblasts captured on a rigid microplate were placed into contact with a fibronectin-coated flexible microplate, then pulled away from it (Figs. 1 and 2). This resulted in the rupture of adhesion between the cell and the fibronectin-coated microplate (Fig. 2). Fibroblasts elongated significantly in this process, but recovered their original morphology within 1–2 min after detachment (Fig. 2C, D). Such shape recovery plus the fact that the cell pattern in phase contrast mode was unaltered (cell lysis is accompanied by a dramatic change in light density, see Thoumine and Ott 1997b) were signs that cells were still alive after adhesive rupture. In a few experiments, we observed the formation of thin filaments (supposedly lipid tethers) between the cell surface and the flexible microplate, but in the majority of cases there was a smooth peeling and a rapid rupture. There was no visible cellular material left behind on the flexible microplate, as judged from bright field and phase contrast images (Fig. 4A), but we hypothesized that fibronectin receptors such as the $\alpha_5\beta_1$ integrin could be uprooted from the membrane. However, we did not observe any specific or localized staining for either α_5 or β_1 integrin subunits on the flexible microplate (Fig. 4B). The observation of stained microplates by epifluorescence is not sufficiently sensitive to detect the uprooting of individual receptors, but probably that of patches. If all the receptors were extracted from the basal surface and remained on the microplate, a diffuse staining would presumably be observed. Control stainings on cells adherent to fibronectin-coated coverslips indicated that the $\alpha_5\beta_1$ integrin was indeed present on the basal fibroblast surface at the time of the experiment (not shown). This receptor is rather insensitive to trypsin at the concentrations used (Akiyama and Yamada 1985), and the cells were allowed to recover from trypsin treatment at 37 °C for 1 h (during which they adhered to the rigid microplate) before the mechanical test. Finally, a bright staining for fibronectin was observed at the location of rupture (Fig. 4C), suggesting that it was not peeled off the substrate. Taken together, these observations suggest that adhesive rupture occurs at the receptor-ligand interface.

Quantification of rupture dynamics

The rupture pattern described below was common to all experimental conditions (different ligand densities and

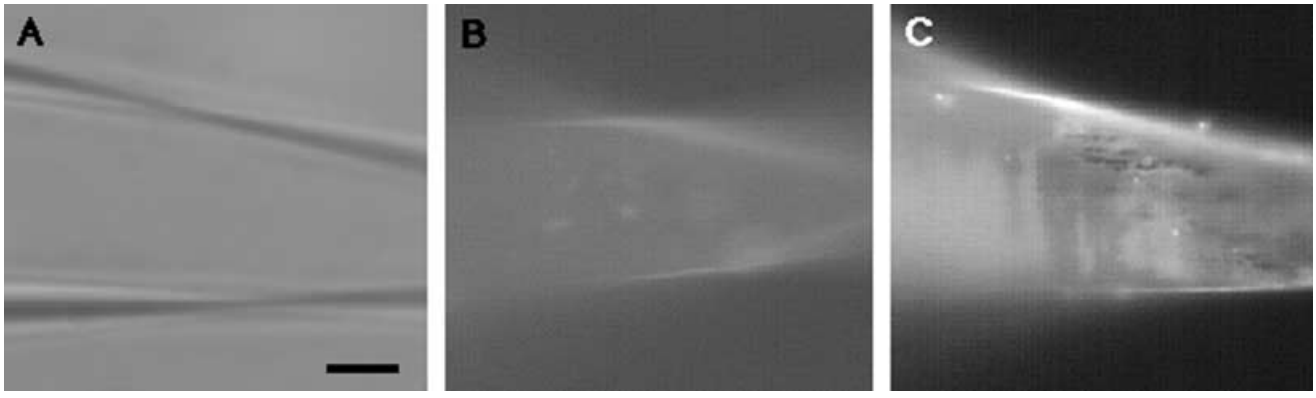

Fig. 4A–C Visualization of the contact zone after rupture. Flexible microplates previously in contact with a cell (middle of each image) are shown from above. **A** Bright field view. **B** Immunofluorescent staining for the α_5 integrin; the pattern is similar for the β_1 integrin, and for control samples (primary antibody replaced by PBS). **C** Staining for fibronectin. These are representative video images of triplicate stainings. The ligand density was 1000 molecules/μm^2 (bath concentration 3 μg/ml) and the pulling velocity 2.5 μm/s, both being intermediary values. *Bar*, 5 μm

pulling velocities). The cell was slightly compressed on the substrate, giving rise to a positive contact diameter $D = 15 \pm 3$ μm ($n = 63$), which did not change much during the adhesion period and was roughly independent of compressive force and fibronectin density (not shown). At time zero, the rigid microplate was moved away at constant velocity. The contact diameter decreased steadily, then dropped rapidly at the time of adhesive rupture (Fig. 5A). The peeling velocity, taken as the derivative of the contact diameter, remained around zero during pulling, and showed a large positive peak around 8 μm/s at the time of rupture (Fig. 5B). The uniaxial force during the attachment period was slightly below zero (between −2 and −20 nN), owing to compression (Fig. 5C, time zero). During pulling, the force increased linearly with time, reached a maximum, then decreased quickly to zero. The initial linear increase in force is likely due to the elastic behavior of fibroblasts at short term (Thoumine and Ott 1997a). When tethers were formed, the drop in force was more progressive (not shown). Adhesion was ligand-specific since the

Fig. 5A–D Quantification of adhesion rupture. **A** Cell-microplate contact diameter, **B** peeling velocity, and **C** uniaxial force are shown over time during the detachment test. The pulling rate was 25 μm in 10 s. Traces obtained from individual cells are shown, representing the average behavior. Microplates were coated with either 3 μg/ml fibronectin (+Fn), or incubated in PBS alone (−Fn). In **C**, the data before the maximum are fitted by a line, whose slope gives the loading rate F'. The graph in **D** shows the diameter (**A**) versus the force (**C**)

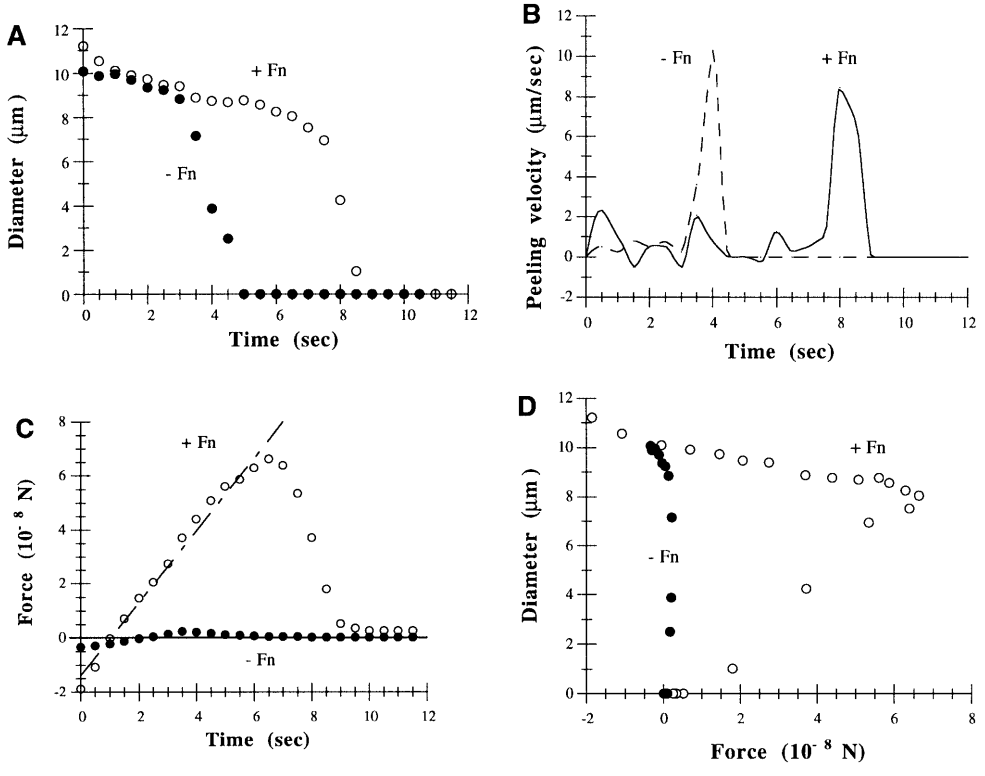

critical rupture time and the maximal force were greater in the presence of fibronectin (Fig. 5A, C, D), whereas only small forces were detected in the absence of fibronectin (maximal force = 4.4 ± 5.1 nN, n = 12 cells). The maximal force for cells incubated with RGD peptides (19 ± 8 nN) was about two-fold smaller than that for control cells (44 ± 40 nN), indicating that integrin receptors were involved in the interaction with fibronectin (Ruoslahti 1996).

Effect of ligand density and loading rate

The density of fibronectin adsorbed on the flexible microplate was varied over two orders of magnitude (30–3000 molecules/μm^2) and the maximal force was quantified for 6–12 cells in each condition. In these experiments, the pulling velocity was maintained constant, i.e. 2.5 μm/s. The maximal adhesive force increased weakly with the number of fibronectin molecules per cell, i.e. the contact area A_c times the ligand density N_L (Fig. 6). The raw data could be fitted by a power function with exponent 0.33 (regression coefficient $r = 0.41$). Next, the time course of the piezo-driven movement was varied by one order of magnitude (3–30 s), while maintaining a constant fibronectin density (incubation concentration 3 μg/ml). The lower time limit was set by data acquisition speed, whereas the upper limit was imposed by active cellular processes and cytoplasmic viscosity (Thoumine and Ott 1997a). The loading rate F' was obtained by a linear fit of the force versus time data in the initial regime, for each individual trace (Fig. 5C). The maximal force was found to increase with F' as a power function with exponent 0.54, $r = 0.78$ (Fig. 7).

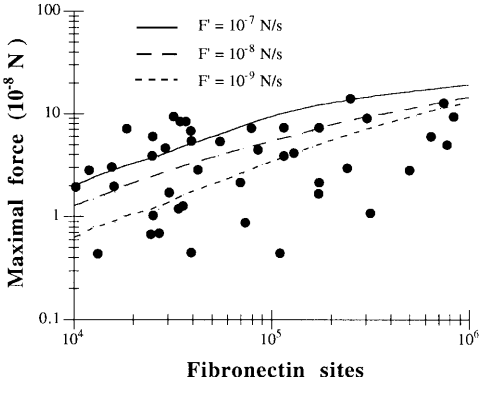

Fig. 6 Rupture force versus number of fibronectin molecules. Four different fibronectin densities were used (coating concentrations 0.3, 1, 3, and 10 μg/ml). The number of fibronectin molecules is the contact area (A_c) times the ligand density (N_L). The pulling rate was 25 μm in 10 s. The maximal force was determined experimentally for each cell (*solid circles*). The *plain* and *dashed curves* are the simulated forces, calculated with $k_{off}^0 = 0.15\ s^{-1}$, $k_{on}^{2D} = 3 \times 10^{-4}\ \mu m^2/s$, $d = 3$ nm, $A_c = 179 \pm 81\ \mu m^2$, and $A_T = 1108 \pm 296\ \mu m^2$ ($n = 43$), for three values of F'. The experimental loading rate was $F' = 1.01 \pm 0.63\ 10^{-8}$ N/s ($n = 43$)

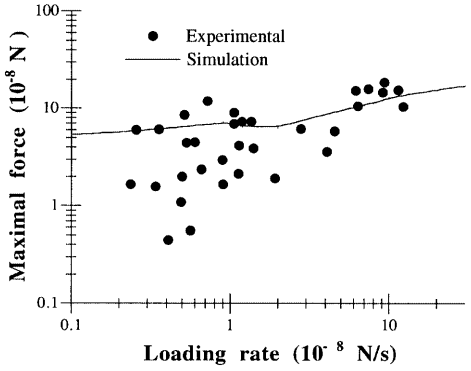

Fig. 7 Critical force versus loading rate. The fibronectin density was maintained constant (1000 molecules/μm^2), and the pulling time was varied between 3 and 30 s. Each *circle* represents an experimental measurement. The *solid line* is the theoretical prediction, obtained after parameter adjustment ($k_{on}^{2D} = 3 \times 10^{-4}\ \mu m^2/s$, $d = 3$ nm), with $A_c = 186 \pm 90\ \mu m^2$ and $A_T = 1098 \pm 303\ \mu m^2$ averaged over the cell population ($n = 32$). Simulations consist in running Eq. (7) for increasing loading rates. Theoretical rupture forces are then obtained by multiplying the time threshold by the loading rate. Such procedure might be responsible for the observed kink in the curve

Interpreting the data with the theory

Both experiments and simulations showed the existence of a maximal force at a critical time, corresponding to adhesion rupture. Comparison of theoretical and experimental forces allowed determination of the two least-known parameters of the model, i.e. the association rate constant (k_{on}^{2D}) and the structural length of the bond (d). Both k_{on}^{2D} and d were varied by factors of 3 within their boundaries (Table 1). The other parameters were measured (ligand density N_L, contact area A_c, total area A_T, and loading rate F') or taken from literature (resting dissociation rate k_{off}^0 and R_T) (Table 1). Because no analytic expression was available to fit the data, an error minimization was carried out as described (Schmidt et al. 1994). For each (k_{on}^{2D}, d) pair, the maximal theoretical force, F_{max}^{sim} was computed and compared to the experimental value, F_{max}^{exp}. The relative difference between the two was squared and summed over all cells ($n = 64$), yielding the following error:

$$\varepsilon = \frac{\sum_{cells} \left(\frac{F_{max}^{exp}}{F_{max}^{sim}} - 1 \right)^2}{n} \qquad (8)$$

For each value of d, the error showed a minimum at a certain k_{on}^{2D} (Fig. 8). The lowest error ($\varepsilon = 0.135$) was obtained for $d = 3$ nm and $k_{on}^{2D} = 3 \times 10^{-4} \mu m^2/s$. Using those values and averaging the other parameters (A_c, A_T) over the cell population, we predicted the relationships between F_{max}^{sim} and the number of ligand molecules, for extreme values of the loading rate F' (Fig. 6), in relatively good agreement with the experimental data. We also computed the theoretical relation between F_{max}^{sim} and F', for a constant fibronectin density. The curve obtained by simulation fell within the upper experimental points, being much higher than the data at low

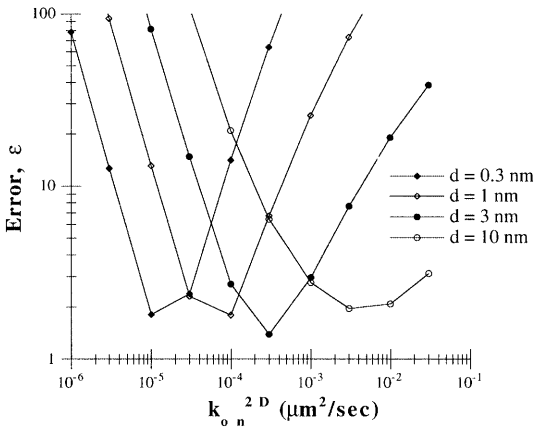

Fig. 8 Error minimization. The error ε characterizes the gap between theoretical and experimental rupture forces (Eq. 8). It is shown versus the association rate constant k_{on}^{2D} for different values of the bond interaction distance d, on a logarithmic plot. Note the existence of a sharp minimum for each curve

F' (Fig. 7). Finally, simulation of the adhesion phase (Eq. 5) predicts that the number of bonds $n = \theta_a R_T$ at the end of the adhesion period is between 1000 (low ligand regime) and 10000 (high ligand density), steady state binding being reached in about 20 s.

Discussion

Comparison with other experimental approaches

We characterized the rupture of adhesion between fibroblasts and fibronectin coated-glass using microplate manipulation, a technique originally designed to probe cell mechanical behavior (Thoumine and Ott 1997a). The method yields high-resolution side-views of the cells, allowing calculation of surface areas. In addition, we computed instantaneous forces at the cell-substrate interface and deduced the loading rate. We also varied the fibronectin density and the pulling velocity; thus most physicochemical variables could be quantified. The main finding was that the force increases linearly with time, then drops sharply at a critical time, giving rise to a maximal force. Rupture forces were in the range of 3×10^{-9} and 2×10^{-7} N, in good agreement with values obtained by detaching cell populations with a laminar shear stress (Mège et al. 1986; Truskey and Pirone 1990; Palecek et al. 1997) or a centrifugal force (Hertl et al. 1984; Thoumine et al. 1996), although certain studies report 10–100 times lower forces (Mohandas et al. 1974; Lotz et al. 1989; Piper et al. 1998). This discrepancy may be attributed to different factors (temperature, ligand density, receptor type and number, adhesion time) which, as shown by the model, can all affect adhesive rupture. The advantage of micromanipulation over flow and centrifugation techniques is that one can directly visualize adhesive rupture and quantify its dynamic properties. On the other hand, because it is tedious and time consuming, one can study only a few cells and has to face a large amount of variability (see Fig. 7). These other techniques are complementary since they can provide statistical information over large numbers of cells. Our method resembles that used by Coman (1944) to separate pairs of normal and transformed cells (cells were pierced with microneedles), although here we do not damage the cells. Micropipet techniques have been used for several years to quantify adhesive forces. In these experiments, a cell is aspirated in a micropipet at increasing pressure levels and the pipet is pulled away until the cell detaches from another cell (Sung et al. 1994; Zhu et al. 1994) or a flat substrate (Tözeren et al. 1992; Sung et al. 1994). One drawback of that approach is that there is no mechanical equilibrium, because the cell penetrates into the pipet while it detaches (Thoumine et al. 1999a, b). In our hands, the aspiration pressure needed to balance adhesive force was so high that it aspirated the whole cell into the micropipet. Moreover, before producing the rupture, one has to adjust the pressure step-by-step, leading to repeated perturbation of the cell, whereas with microplates there is just one pulling test. Despite these differences, the rupture forces of fibroblasts interacting with fibronectin-coated glass as well as the decrease in contact diameter over time found here are similar to those obtained by micropipet (respectively Sung et al. 1994 and Tözeren et al. 1992).

Validity of the model

The deterministic theoretical analysis built by extending on previous work (Cozens-Roberts et al. 1990) yields the mean number of ligand-receptor bonds over time. In the adhesion phase, the bond number increases to an equilibrium value. Consistent with the deterministic framework, we found that many bonds ($n > 10^3$) were formed in fibroblast-fibronectin adhesion, at relatively long contact times (5 min). This agrees with actual measurements of bond number at adhesive contacts (Dustin et al. 1996). Experiments with optical tweezers also using 3T3 fibroblasts interacting with fibronectin-coated glass, showed that the number of bonds at short term ($1 < t < 16$ s) was very low, i.e. $n < 7$ (Thoumine et al. 2000), and in that case the data had to be interpreted using a probabilistic formalism (Cozens-Roberts et al. 1990). In the presence of an external load, here increasing linearly with time, the theory shows that all the bonds break at once as soon as the force exceeds a critical value, in agreement with experiments. This is because each time a bond breaks, there are fewer bonds to sustain the same force, leading to a catastrophic event. Critical forces were also observed in flow and centrifugation studies (Mohandas et al. 1974; Hertl et al. 1984; Thoumine et al. 1996). In other reports the force dependence is smoother (Truskey and Pirone 1990), reflecting either population heterogeneity (Piper

et al. 1998) or probabilistic fluctuations at the bond level (Cozens-Roberts et al. 1990). It may be possible to relax some of our assumptions (e.g. those of constant contact area A_c, 1:1 stochiometry of the ligand-receptor reaction, absence of diffusion of receptors in the contact zone, homogeneous distribution of the force among all bonds), but as such the model already captures the essential features of the experiments.

Other theoretical approaches, based on a continuum analysis of membrane mechanics at the adhesive zone, lead to the predictions that peeling velocity undergoes an overshoot and damped oscillations prior to reaching a steady state value (Dembo et al. 1988; Ward et al. 1995). This is consistent with our experiments, in which the peeling velocity fluctuates around zero during pulling and reaches a peak at the time of adhesive breakage. The force data agree well with predicted values, i.e. on the order of 10^{-7} N, for a fracture mechanism where focal contacts are considered as mechanically rigid entities (Ward and Hammer 1993). The relationship between the critical force and the number of available fibronectin molecules (Fig. 6) is also well described by such models: our experiments fall between a low ligand density regime, characterized by linear increase in force, and a high ligand density regime, where the critical tension increases only moderately (Ward et al. 1995). The distinction between different models is difficult at this stage because of scatter in the data. Generally, theoretical treatments of cell adhesion are more accurate for short-term experiments (time scale of seconds) which deal with only a few ligand-receptor bonds. At longer term (hours), where biological processes are more complex (involving, for example, receptor aggregation, connection to the cytoskeleton, and cell deformation), such descriptions become a difficult task, having to deal with many unknowns. For the middle term situation (several minutes) described here, a simple model of bond dynamics containing a minimal number of adjustable parameters and giving a straightforward representation of adhesion seems reasonably appropriate.

Biology of adhesion rupture

Rupture of adhesion between cells and their substrate may occur at various locations when one pulls on adhesive sites, depending presumably on many factors (extent of receptor aggregation, bond affinity, rate of force, etc.). Reversible formation and rupture of receptor-ligand bonds occurs during leukocyte rolling on endothelial cells (Kaplanski et al. 1993; Alon et al. 1995). In addition, receptor extraction may take place during separation of antibody-agglutinated red blood cells (Evans et al. 1991); the force, around 20 pN, corresponds to that holding receptors in the lipid bilayer, and is rather independent of the type of receptor. In other cases there is breakage of integrin-cytoskeleton links, the integrin-ligand bond remaining intact; for example, migrating cells leave behind their trailing edge cytoplasmic material, rich in integrins but lacking vinculin (Chen 1981; Regen and Horwitz 1992). Furthermore, microspheres exhibiting retrograde movement on the dorsal surface of lamellae can be detached from the actin cortex, although they stay anchored to the membrane (Choquet et al. 1997). Under other conditions, dissociation of the lipid bilayer from the underlying cytoskeletal network can occur, resulting in the formation of lipid tethers (Zhu et al. 1994; Dai and Sheetz 1995). Stripping of the plasma membrane has also been reported, for instance membrane material is left behind onto the substrate when cells are detached by centrifugation (Hertl et al. 1984) or when permeabilized cells are induced to retract by ATP treatment (Thoumine and Ott 1996). Here, adhesive rupture seemed to occur at the integrin-fibronectin interface because fibronectin, which is known to strongly adsorb to glass (Haas and Culp 1982), was still present on the microplate after fracture. Moreover, no detectable membrane material was left behind on the substrate. This gives credit to our model which emphasizes ligand-receptor dynamics. Although specific adhesion was significantly reduced by RGD peptides, we do not know precisely which receptor was involved in fibronectin recognition in the present study. It is possible that several integrins were involved in binding fibronectin, in which case the model coefficients would reflect average properties (Thoumine et al. 2000). Finally, the fact that forces to rupture adhesion are of the same order of magnitude as those involved in fibroblast traction (Harris 1980; Oliver et al. 1995; Thoumine and Ott 1997a) confirms that the mechanical balance between cytoskeletal tension and adhesiveness plays a major role in cell morphology and movement (Lauffenburger and Horwitz 1996; Palecek et al. 1997).

Physical relevance of the parameters

Comparison of the simulations with experimental data allowed estimation of two unknown parameters, i.e. the association rate constant ($k_{on}^{2D} = 3 \times 10^{-4}\,\mu m^2/s$) and the structural length of the bond ($d = 3$ nm). In a companion paper, we studied the short-term adhesion of fibroblasts to fibronectin-coated glass with optical tweezers, and computed the kinetic rates k_{on} and k_{off} (Thoumine et al. 2000). We found that k_{on} increased in a logarithmic manner with compression on the cell in the range of 0–60 pN, whereas k_{off} was unaffected. The compressive forces imposed here during the adhesion phase were around $1–3 \times 10^{-8}$ N, so we could not ignore their effect on k_{on}. Indeed, the association rate constant found from error minimization was approximately 10 times larger than its value at low compression. The increase in k_{on} cannot be explained by extrapolation from the logarithmic relation, which thus seems valid only at low forces (Thoumine et al. 2000). More likely, compressive forces are large enough to increase the actual contact area by smoothing out the basal surface (unfolding wrinkles), thereby allowing greater accessibility

of receptors to immobilized fibronectin. Indeed, the surface stiffness has been estimated to 30 pN/nm (Lo et al. 1998), thus the decrease in cell height in response to 3×10^{-8} N is on the order of 1 μm, in agreement with our observations.

Our data are consistent with an exponential dependence of the dissociation rate versus the tensile force on the bond (Eq. 6). This phenomenological relationship was originally postulated by Bell (1978) and used in several studies (Hammer and Lauffenburger 1987; Cozens-Roberts et al. 1990; Alon et al. 1995; Piper et al. 1998). The structural length d may be interpreted as the width of the binding pocket, in the energy profile of the ligand-receptor interaction (Evans 1985; Evans and Ritchie 1997). It should be on the order of 0.3–0.5 nm, a typical range for the hydrophobic forces involved in protein-protein interaction (Bell 1978; Erickson 1994). Here we found $d = 3$ nm, a high value which may reflect the fact that fibronectin can stretch over tens of nanometer distances under forces of several piconewtons, by unfolding of type III domains (Erickson 1994). With an activation energy of $E_a = 20\ k_B T$, and an individual separation strength $f_a = 20$ pN (Thoumine et al. 2000), one can compute a characteristic length for the fibronectin-integrin bond, $E_a/f_a = 4$ nm, very close to the value reported here. The interaction distance of the selectin-carbohydrate ligand bond, as assessed by flow (Alon et al. 1995) or centrifugation experiments (Piper et al. 1998), was reported to be in the range of 0.03–0.05 nm, thus 100 times smaller than the one found here for the fibronectin-integrin bond. This may reflect an essential difference between integrins and selectins. Because the significance of the structural length is not straightforward, one may prefer to define an empirical force parameter, $f_0 = k_B T/d$, here close to 1 pN.

Finally, the model was not very good at predicting the relationship between rupture force and loading rate, especially at low F' (Fig. 7). One explanation of such behavior is that there is significant force relaxation at slow pulling rates, e.g. 30 s, because of viscous behavior. Indeed, this value is close to the characteristic relaxation time for chick fibroblasts, i.e. 1 min (Thoumine and Ott 1997a). Another possibility is that the kinetic parameters depend on the loading rate. For example, one may introduce a logarithmic prefactor, e.g. $\ln(F'/F'_0)$, in Eq. (6), as previously suggested (Evans et al. 1991; Evans and Ritchie 1997). With such a modified relation, one may be able to model the experimental dependence of critical force versus loading rate. We did not attempt to do so because it would introduce another unknown parameter (e.g. the reference loading rate F'_0), and thereby complicate the interpretation.

Conclusion

We measured forces to rupture adhesion between fibroblasts and fibronectin-coated glass with a recent micromanipulation technique, which we interpreted using a deterministic model of bond kinetics. This led to the estimation of some physical properties of the fibronectin-integrin bond, in particular the association rate constant and structural length of the interaction. Other parameters, the dissociation rate, strength, and energy well of the bond, are available from a companion study (Thoumine et al. 2000). Overall, this constitutes an integrated approach to the biophysical characterization of a particular receptor-ligand pair, which plays an important role in cell interaction with the extracellular matrix.

Acknowledgements This work was supported by funds from our own institute. We thank M. Walisewsky for help with electronics, A. Terrier for advice on Mathematica, N. Caille for building the system to transfer cells to the incubator, A. Kottelat for expert technical assistance on carrying out initial tests, O. Cardoso for the computer macro to calculate cell area, A. Ott for continuous support, and T.M. Quinn for fruitful discussions.

References

Akiyama SK, Yamada SS (1985) The interaction of plasma fibronectin with fibroblastic cells in suspension. J Biol Chem 260: 4492–4500

Alon R, Hammer DA, Springer TA (1995) Lifetime of the P-selectin-carbohydrate bond and its response to tensile force in a hydrodynamic flow. Nature 374: 539–542

Bell GI (1978) Models for the specific adhesion of cells to cells. A theoretical framework for adhesion mediated by reversible bonds between cell surface molecules. Science 200: 618–627

Bell GI, Dembo M, Bongrand P (1984) Cell adhesion, competition between non specific repulsion and specific bonding. Biophys J 45: 1051–1064

Bongrand P, Claesson PM, Curtis ASG (eds) (1994) Studying cell adhesion. Springer, Berlin, Heidelberg, New York

Burridge K, Chrzanowska-Wodnicka M (1996) Focal adhesions, contractility and signaling. Annu Rev Cell Dev Biol 12: 463–519

Chen WT (1981) Mechanism of retraction of the trailing edge during fibroblast movement. J. Cell Biol. 90: 187–200

Choquet D, Felsenfeld DP, Sheetz MP (1997) Extracellular matrix rigidity causes strengthening of integrin-cytoskeletal linkages. Cell 88: 39–48

Codogno P, Doyennette-Moyne MA, Aubery M (1987) Evidence for a dual mechanism of chick embryo fibroblast adhesion on fibronectin and laminin substrata. Exp Cell Res 169: 478–489

Coman DR (1944) Decreased mutual adhesiveness, a property of cells from squamous carcinomas. Cancer Res 4: 625–629

Cozens-Roberts C, Lauffenburger DA, Quinn JA (1990) Receptor-mediated cell attachment and detachment kinetics. I. Probabilistic model and analysis. Biophys J 58: 841–856

Crowley E, Horwitz AF (1995) Tyrosine phosphorylation and cytoskeletal tension regulate the release of fibroblast adhesions. J Cell Biol 131: 525–537

Dai J, Sheetz MP (1995) Mechanical properties of neuronal growth cone membranes studied by tether formation with laser optical tweezers. Biophys J 68: 988–996

Davies PF, Robotewskyj A, Griem ML (1994) Quantitative studies of endothelial cell adhesion. Directional remodeling of focal adhesion sites in response to flow forces. J Clin Invest 93: 2031–2038

Dembo M, Torney DC, Saxman K, Hammer D (1988) The reaction-limited kinetics of membrane-to-surface adhesion and detachment. Proc R Soc Lond B 234: 55–83

Duband JL, Nuckolls GH, Ishihara A, Hasegawa T, Yamada KM, Thiery JP, Jacobson K (1988) Fibronectin receptor exhibits

high lateral motility in embryonic locomoting cells but is immobile in focal contacts and fibrillar streaks in stationary cells. J Cell Biol 107: 1385–1396

Dustin ML, Ferguson LM, Chan PY, Springer TA, Golan DE (1996) Visualization of CD2 interaction with LFA-3 and the determination of the two-dimensional dissociation constant for adhesion receptors in a contact area. J Cell Biol 132: 465–474

Erickson HP (1994) Reversible unfolding of fibronectin type III and immunoglobulin domains provides the structural basis for stretch and elasticity of titin and fibronectin. Proc Natl Acad Sci USA 91: 10114–10118

Evans EA (1985) Detailed mechanics of membrane-membrane separation. II. Discrete kinetically trapped molecular cross-bridges. Biophys J 48: 185–192

Evans E, Ritchie K (1997) Dynamic strength of molecular adhesion bonds. Biophys J 72: 1541–1555

Evans E, Berk D, Leung A (1991) Detachment of agglutinin-bonded red blood cells. I. Forces to rupture molecular-point attachments. Biophys J 59: 838–848

Haas R, Culp LA (1982) Properties and fate of plasma fibronectin bound to the tissue culture substratum. J Cell Physiol 113: 289–297

Hammer DA, Lauffenburger DA (1987) A dynamical model for receptor-mediated cell adhesion to surfaces. Biophys J 52: 475–487

Harris AK, Wild P, Stopak D (1980) Silicone rubber substrata: a new wrinkle in the study of cell locomotion. Science 208: 177–179

Hertl W, Ramsey WS, Nowlan ED (1984) Assesment of cell-substrate adhesion by a centrifugal method. In Vitro 20: 796–801

Hubbe MA (1981) Adhesion and detachment of biological cells in vitro. Prog Surf Sci 11: 65–138

Huttenlocher A, Sandborg RR, Horwitz AF (1995) Adhesion in cell migration. Curr Opin Cell Biol 7: 697–706

Hynes RO (1992) Integrins: versatility, modulation, and signaling in cell adhesion. Cell 69: 11–25

Ingber D (1991) Integrins as mechanochemical transducers. Curr Opin Cell Biol 3: 841–848

Kaplanski G, Farnarier C, Tissot O, Pierres A, Benoliel AM, Alessi MC, Kaplanski S, Bongrand P (1993) Granulocyte-endothelium initial adhesion: analysis of transient binding events mediated by E-selectin in a laminar shear flow. Biophys J 64: 1922–1933

Kreis TE, Birchmeier W (1980) Stress fiber sarcomeres of fibroblasts are contractile. Cell 22: 555–561

Lauffenburger DA, Horwitz AF (1996) Cell migration: a physically integrated molecular process. Cell 84: 359–369

Lauffenburger DA, Linderman JJ (1993) Receptors: models for binding, trafficking, and signaling. Oxford University Press, New York

Lo CM, Glogauer M, Rossi M, Ferrier J (1998) Cell-substrate separation: effect of applied force and temperature. Eur Biophys J 27: 9–17

Lotz MM, Burdsal CA, Erickson HP, McClay DR (1989) Cell adhesion to fibronectin and tenascin: quantitative measurements of initial binding and subsequent strengthening response. J Cell Biol 109: 1795–1805

McClay DR, Wessel GM, Marchase RB (1981) Intercellular recognition: quantitation of initial binding events. Proc Natl Acad Sci USA 78: 4975–4979

McCloskey MA, Poo M (1986) Contact-induced redistribution of specific membrane components: local accumulation and development of adhesion. J Cell Biol 102: 2185–2196

Mège JL, Capo C, Benoliel AM, Bongrand P (1986) Determination of binding strength and kinetics of binding initiation. Cell Biophys 8: 141–160

Michl J, Pieczonka MM, Unkeless JC, Bell GI, Silverstein SC (1983) Fc receptor modulation in mononuclear phagocytes maintained on immobilized immune complexes occurs by diffusion of the receptor molecule. J Exp Med 157: 2121–2139

Mohandas N, Hochmuth RM, Spaeth EE (1974) Adhesion of red cells to foreign surfaces in the presence of flow. J Biomed Mater Res 8: 119–136

Mosher DF (ed) (1989) Fibronectin. Academic Press, San Diego

Oliver T, Dembo M, Jacobson K (1995) Traction forces in locomoting cells. Cell Motil Cytoskel 31: 225–240

Palecek SP, Loftus JC, Ginsberg MH, Lauffenburger DA, Horwitz AF (1997) Integrin-ligand binding properties govern cell migration speed through cell-substratum adhesiveness. Nature 385: 537–540

Piper JW, Swerlick RA, Zhu C (1998) Determining force dependence of two-dimensional receptor-ligand binding affinity by centrifugation. Biophys J 74: 492–513

Regen CM, Horwitz AF (1992) Dynamics of β1 integrin-mediated adhesive contacts in motile fibroblasts. J Cell Biol 119: 1347–1359

Ruoslahti E (1996) RGD and other recognition sequences for integrins. Annu Rev Cell Dev Biol 12: 697–715

Schmidt CE, Chen T, Lauffenburger DA (1994) Simulation of integrin-cytoskeletal interactions in migrating fibroblasts. Biophys J 67: 461–474

Sheetz MP (1993) Glycoprotein motility and dynamic domains in fluid plasma membranes. Annu Rev Biophys Biomol Struct 22: 417–431

Sung KLP, Kwan MK, Maldonado F, Akeson WH (1994) Adhesion strength of human ligament fibroblasts. J Biomech Eng 116: 237–242

Thoumine O, Ott A (1996) Influence of adhesion and cytoskeletal integrity on fibroblast traction. Cell Motil Cytoskel 35: 269–280

Thoumine O, Ott A (1997a) Time scale dependent viscoelastic and contractile regimes in fibroblasts probed by microplate manipulation. J Cell Sci 110: 2109–2116

Thoumine O, Ott A (1997b) Comparison of the mechanical properties of normal and transformed fibroblasts. Biorheology 34: 309–326

Thoumine O, Ott A, Louvard D (1996) Critical centrifugal forces induce adhesion rupture or structural reorganization in cultured cells. Cell Motil Cytoskel 33: 276–287

Thoumine O, Cardoso O, Meister JJ (1999a) Changes in the mechanical properties of fibroblasts during spreading: a micromanipulation study. Eur Biophys J 28: 222–234

Thoumine O, Ott A, Cardoso O, Meister JJ (1999b) Microplates: a new tool for manipulation and mechanical perturbation of individual cells. J Biochem Biophys Methods 39: 47–62

Thoumine O, Kocian P, Kottelat A, Meister JJ (2000) Short term binding of fibroblasts to fibronectin: optical tweezers experiments and probabilistic analysis. Eur Biophys J 29: 398–408

Tözeren A (1990) Cell-cell, cell-substrate adhesion: theoretical and experimental considerations. J Biomech Eng 122: 311–318

Tözeren A, Mackie LH, Lawrence MB, Chan PY, Dustin ML, Springer T (1992) Micromanipulation of adhesion of phorbol 12-myristate-13-acetate-stimulated T lymphocytes to planar membranes containing intercellular adhesion molecule-1. Biophys J 63: 247–258

Truskey GA, Pirone JS (1990) Effect of fluid shear stress upon cell adhesion to fibronectin-treated surfaces. J Biomed Mater Res 24: 1333–1353

Ward MD, Hammer DA (1993) A theoretical analysis for the effect of focal contact formation on cell-substrate attachment strength. Biophys J 64: 936–959

Ward MD, Dembo M, Hammer DA (1995) Kinetics of cell detachment: effect of ligand density. Ann Biomed Eng 23: 322–331

Zhu C, Williams TE, Delobel J, Xia D, Offermann MK (1994) A cell-cell adhesion model for the analysis of micropipette experiments. In: Mow VC, Guilak F, Tran-Son-Tay R, Hochmuth RM (eds) Cell mechanics and cellular engineering. Springer, Berlin Heidelberg New York, pp 160–181